

HI Observations of the Ca II absorbing galaxies Mrk 1456 and SDSS J211701.26-002633.7

B. Cherinka¹, R.E. Schulte-Ladbeck¹, and J. L. Rosenberg²

Department of Physics & Astronomy, University of Pittsburgh, Pittsburgh, PA 15260

Department of Physics and Astronomy, George Mason University, Fairfax, VA 22030

bac29@pitt.edu

ABSTRACT

In an effort to study Damped Lyman Alpha galaxies at low redshift, we have been using the Sloan Digital Sky Survey to identify galaxies projected onto QSO sightlines and to characterize their optical properties. For low redshift galaxies, the HI 21cm emission line can be used as an alternate tool for identifying possible DLA galaxies, since HI emitting galaxies typically exhibit HI columns that are larger than the classical DLA limit. Here we report on follow-up HI 21 cm emission line observations of two DLA candidates that are both low-redshift spiral galaxies, Mrk 1456 and SDSS J211701.26-002633.7. The observations were made using the Green Bank and Arecibo Telescopes, respectively. Analysis of their HI properties reveal the galaxies to be about one and two M_{HI}^* galaxies, respectively, and to have average HI mass, gas-richness, and gas mass fraction for their morphological types. We consider Mrk 1456 and SDSS J211701.26-002633.7 to be candidate DLA systems based upon the strength of the CaII absorption lines they cause in their QSO's spectra, and impact parameters to the QSO that are smaller than the stellar disk. Compared to the small numbers of other HI-detected DLA and candidate DLA galaxies, Mrk 1456 and SDSS J211701.26-002633.7 have high HI masses. Mrk 1456 and SDSS J211701.26-002633.7 have also been found to lie in galaxy groups that are high in HI gas mass compared to the group containing SBS 1543+593, the only DLA galaxy previously known to be situated in a galaxy group. When compared with the expected properties of low- z DLAs from an HI-detected sample of galaxies, Mrk 1456 and SDSS J211701.26-002633.7 fall within the ranges for impact parameter and M_B ; and the HI mass distribution for the HI-detected DLAs agrees with that of the expected HI mass distribution for low- z DLAs. Our observations support galaxy-evolution models in which high mass galaxies make up an increasing contribution to the DLA cross-section at lower redshifts. We also report on the 21 cm line emission of Mrk 1457, a Seyfert galaxy observed within the beam of the Green Bank Telescope.

Subject headings: galaxies: individual(Mrk 1456, Mrk 1457, SDSS J211701.26-002633.7) — quasars: absorption lines — radio lines: galaxies

1. Introduction

Damped Lyman Alpha (DLA) absorbers are the primary reservoir of cool, neutral gas in the Universe and the ability to detect them easily over a wide range of redshifts make them an important tracer of the evolution of gas in galaxies or protogalaxies over cosmic time. DLA systems are identified at redshifts $0 < z < 6$ in the

spectra of QSOs (Wolfe et al. 2005). Identified from the strong $n=1$ to $n=2$ absorption line of HI, the detection of these absorption-selected objects depends primarily on the brightness of the background QSO rather than on emission from stars or gas. It is noteworthy that the column density of $N_{HI} > 10^{20.3}$ atoms cm^{-2} , that defines a DLA (Wolfe et al. 1986), is similar to the threshold column density required for

the onset of star formation in the local Universe (Kennicutt 1998). DLAs, then, should be associated with present-day visible galaxies (Wolfe et al. 1986; Prochaska & Wolfe 1997; Boissier et al. 2003). However, difficulty still remains in connecting observations of high-redshift DLAs with those of low-redshift DLAs, as well as connecting galaxy-evolution simulations with DLA observations. Simulations at low redshift by Okoshi & Nagashima (2005) and Nagamine et al. (2007) indicate that the DLA incidence is dominated by more compact, faint galaxies with a narrow impact parameter distribution (<3 kpc), rather than by large disk galaxies. Observationally, low redshift DLA systems have been shown to consist of galaxies spanning a wide range of luminosities, surface brightnesses, impact parameters, and morphologies (Le Brun et al. 1997; Chen & Lanzetta 2003; Rao et al. 2003). At higher redshifts, the associated host galaxy to the DLA has proven difficult to identify due to the high brightness contrast between the quasar and the absorbing galaxy. Another issue in the identification of the host galaxy at high redshift is the fact that one can no longer detect faint galaxies that may be intercepting your sightline. This may cause a misidentification of the host galaxy, especially in high density regions like groups. This may contribute to the larger impact parameters being measured for high redshift systems. Christensen et al. (2007) identified candidate hosts to high-redshift ($2 < z < 4$) DLAs through IFU observations of the Ly α -emission line. While they have a small sample size, they find an average impact parameter of 16 kpc, and suggest the distribution of HI clouds for DLAs extends far beyond the optical sizes of dwarfs. Simulations by Gardner et al. (2001) resulted in larger impact parameters (10-15 kpc) for $2 < z < 4$.

Selecting systems by identifying damped Lyman- α absorption provides only a pencil-beam examination of the gas content of DLA host galaxies, missing the full gas content that can be probed. An alternative then, to searching for gas through Lyman-alpha absorption, is to use the 21 cm emission line, which probes the global gas content in galaxies, to search for systems that are likely to show damped Lyman- α profiles if there were a background source. The HI hyperfine structure line at 21 cm is very weak, and its detection is

currently limited to low redshifts. HI 21 cm observations probe the cold, neutral Hydrogen gas in a galaxy and come in two forms, 21 cm absorption and 21 cm emission. 21 cm absorption, like other absorption-line probes, provides a pencil-beam look at the HI content of a galaxy. It requires a background radio-loud point source and allows for a direct determination of N_{HI} . 21 cm line emission is a probe of the gas contained within the beam of the telescope, smoothed according to the spatial resolution of the telescope. The resulting HI emission spectrum reveals the global HI content of the galaxy and allows for determination of the HI mass while maps show the distribution and cross-sections of HI gas around a galaxy. Estimates of the gas column density within the beam can be obtained by the ratio of the HI flux to the area covered. A probe of emission might reveal an average HI column above $10^{20.3}$, however this is over a much larger area than that probed by absorption, therefore there is no guarantee that a QSO probe will reveal a DLA at every position within the emission beam. Emission-line probes above $10^{20.3}$ only say that somewhere they generally exceed the DLA limit. Ryan-Weber et al. (2003) showed that HI-emission selected galaxies generally show more cross-section at higher column densities than they do at lower column densities and most exhibit column densities that are above the DLA limit. The HI-emission-selected galaxies are consistent with the hypothesis that the local galaxy population can explain the properties of the local DLAs. Rosenberg & Schneider (2003), and Ryan-Weber et al. (2003) studied the expected properties of the $z=0$ DLA population using blind 21 cm emission surveys, and found that, while a large fraction of HI-selected galaxies are dwarf or low surface brightness galaxies, there is no need for an optically invisible population of galaxies to explain the HI population or to contribute significantly to the DLA cross section.

There are presently only a small number of (sub) DLAs or DLA candidates known at low-redshift and an even smaller number that have HI measured in emission. It should be noted that a DLA (and sub-DLA) system is classically defined as a system with an observed $N_{HI} > 10^{20.3}$ atoms cm^{-2} ($10^{19.0}$ $\text{cm}^{-2} < N_{HI} < 10^{20.3}$ cm^{-2}) measured via the Ly- α absorption line. The term ‘‘candidate DLA’’ is used

to describe all galaxies that have $N_{\text{HI}} > 10^{20.3}$ atoms cm^{-2} measured through other means, or those with no N_{HI} measurement but meet the criteria of various metal-DLA relationships (e.g. Mg II, Ca II, Na I). Zwaan et al. (2005) compared the properties of 20 low-redshift ($z < 1$) DLA/sub-DLA galaxies with a sample of local, optically selected galaxies studied in HI 21 cm. Only 2 of the 20 DLAs, SBS 1543+593 and NGC 4203, have measured HI 21 cm emission. One other DLA, the absorber towards the QSO OI 363, and two sub-DLAs, the absorbers towards the QSOs PKS 0439-433 and PG 1216+069, have been searched for 21 cm emission. We use the HI observations of these objects, along with the ones reported here, to further investigate the properties of DLAs at $z=0$ and expand on the number of DLAs or candidates known at low- z with HI 21 cm emission measurements.

Table 1 lists the HI and optical properties of the known/candidate DLAs. A summary of the HI 21 cm observations of these five known/candidate DLAs is as follows. The $z=0.009$ dwarf galaxy SBS 1543+593 has an HI column density of $\log N_{\text{HI}}=20.41$ (Bowen et al. 2005) as measured by the Lyman α line, while Chengalur & Kanekar (2002) find a column density of $\log N_{\text{HI}} = 20.69$ from the 21 cm emission mapped at the position of the QSO. The $z=0.004$ S0 galaxy NGC 4203 was first mapped at 21 cm before the presence of the background QSO Ton 1480 was revealed by X-ray observations. The HI absorption in the X-ray spectrum of Ton 1480 suggests a sufficiently high column density ($\log N_{\text{HI}} = 20.34$) to make this system a candidate DLA. Another known DLA, the $z=0.0912$ absorber towards B 0738+313 (OI 363), has been searched for 21 cm emission but was undetected (Lane et al. 2000). Two sub-DLA's have also been searched for 21 cm emission. The $z=0.101$ absorber towards PKS 0439-433 was thought to be a candidate DLA system based on its X-ray spectrum but measurement of the Lyman α line (Chen et al. 2005) revealed a column density ($\log N_{\text{HI}} = 19.85 \pm 0.04$) just below the limit for DLAs and it was undetected in 21 cm emission (Kanekar et al. 2001). Briggs & Barnes (2006) report a weak 21 cm emission detection along the line of sight towards the QSO PG 1216+069, which is consistent with the velocity of the $z=0.0063$ sub-DLA absorber.

In this paper we present the 21 cm emission detection of Mrk 1456 with the Green Bank Telescope (GBT) and of SDSS J211701.26-002633.7 with the Arecibo telescope¹. Section 2 describes the sample selection, observations, data reductions and analysis. In section 3, we discuss the HI properties of our sample and compare them to HI-detected DLAs and HI-selected galaxies. We adopt a cosmology of $H_0=71 \text{ km s}^{-1} \text{ Mpc}^{-1}$, $\Omega_m=0.27$, $\Omega_\Lambda=0.73$ throughout this paper.

2. Observations and Data Analysis

2.1. Sample Selection and Optical Data

A search was made in the Sloan Digital Sky Survey (SDSS) for candidate DLAs by cross-referencing *known* spectroscopic galaxies with the SDSS Data Release 5 (DR5) QSO catalog Schneider et al. (2007), creating a subset of galaxy-QSO pairs. The motivation behind this approach was spawned by the difficulty of identifying DLA host galaxies at both high and low redshifts. The galaxy-QSO pairs were further trimmed by requiring the impact parameters to be less than twice the Petrosian radius of the galaxy, and that $z_{\text{QSO}} > z_{\text{gal}}$. Twice the Petrosian radius was chosen as HI disks have typically been shown to extend anywhere from 1.5 - 2.0 times the optical radius for spiral galaxies (Cayatte et al. 1994; Broeils & Rhee 1997) and we adopted this cut-off to ensure inclusion of a significant amount of HI in the matching process. As the SDSS is a magnitude limited survey (Strauss et al. 2002), our selection method favors giant over dwarf DLA candidates and thus may tend to select high HI mass galaxies. Mrk 1456 and SDSS J211701.26-002633.7 (SDSS 21-00 for brevity) were selected from this set because the background QSOs are within the stellar disks of the galaxy. Mrk 1456 has an impact parameter, $b=4.9$ kpc, compared with the galaxy's r-band Petrosian radius, $r=7.1$ kpc. For SDSS 21-00, $b=5.7$ kpc while $r=7.5$ kpc. These values are both less than the median impact parameters for DLA hosts ($b < 8.0$ kpc) as found by Zwaan et al. (2005). The SDSS redshifts reported for Mrk 1456, Mrk 1457, and SDSS 21-

¹The Arecibo Observatory is part of the National Astronomy and Ionosphere Center, which is operated by Cornell University under a cooperative agreement with the National Science Foundation.

00 throughout the paper are optical emission line redshifts.

Mrk 1456 and SDSS 21-00 were chosen for follow-up HI observations because they are strong DLA candidates that are within the redshift limits of HI 21 cm observations. The beam of our HI observations also included Mrk 1457 so we present the data for this galaxy as well.

Direct measurement of the damped Lyman- α line in low- z systems requires UV spectroscopy from space, which has not been carried out on the two QSOs in this study. However, the small QSO impact parameters, and the strength of the Ca II doublets ($\lambda\lambda 3934, 3969$) in both Mrk 1456 and SDSS 21-00 indicate that they are likely to be DLAs. Wild & Hewett (2005) and Wild et al. (2006) have estimated that systems with a rest EW($\lambda 3934$) $\geq 0.5 \text{ \AA}$ have a number density $\sim 20\text{--}30\%$ of DLAs and those with EW $\geq 0.68 \text{ \AA}$ are highly likely to be a subset of the DLA population. Nestor et al. (2008) note that while strong Ca II absorbers are likely to be DLAs, not all DLAs will have strong Ca II EWs. König et al. (2006) reported a Ca II K EW of $1.24 \pm 0.15 \text{ \AA}$ for Mrk 1456, well above the threshold for DLA candidates. For SDSS 21-00, we measure a rest Ca II K EW of $1.1 \pm 0.2 \text{ \AA}$, also above threshold. The Ca II EW measurements for both Mrk 1456 and SDSS 21-00 were made by fitting Gaussians to the lines using a local fit to the continuum.

König et al. (2006) reported on Mrk 1456 as a typical, L_* , giant spiral galaxy with a spectrum of an Sc type disk galaxy. For SDSS 21-00, comparison of its spectrum with the templates of Kennicutt (1992) and using the inverse concentration index and u-r color (Park & Choi 2005; Shimasaku et al. 2001) suggests that it is an Sb type spiral galaxy. A morphological examination of the optical image for SDSS 21-00 shows it is a late-type disk galaxy. Mrk 1457 is classified as a Seyfert 2 galaxy in NED² and lies $2.3'$ (2.2 kpc) south of Mrk 1456.

The inclinations, i , of each galaxy were computed using the minor-to-major axis ratio in the r band measured from an exponential fit to the profile, measured out to a radius of three times the effective radius. This gives 45° , 25° , and 52° , for the inclinations of Mrk 1456, Mrk 1457, and

SDSS 21-00 respectively.

We use the SDSS g and r photometry to calculate the galaxies' absolute magnitudes and luminosities and then transform to Johnson-Morgan Cousins B using the Smith et al. (2002) transformation laws. The absolute B-band magnitudes reported here were converted to the AB zeropoint system, corrected for galactic extinction (Schlegel et al. 1998), and k-corrected. In order to make a consistent comparison of Mrk 1456 and SDSS 21-00 to objects published in the literature, we use k-corrections from Poggianti (1997). With the galaxy inclinations given above, and the HI velocity widths listed in Table 3, we correct for internal extinction using the method of Tully et al. (1998). All magnitudes and luminosities are listed in Table 2. Assuming $M_B^* = -20.9$ (Marinoni et al. 1999), Mrk 1456 and SDSS 21-00 are $\sim 0.5 L_B^*$ galaxies, and Mrk 1457 is a $1.4 L_B^*$ galaxy.

Following the prescription of Hopkins et al. (2003), we derive star-formation rates (SFR) for our objects and for those literature objects for which the data were available or could be calculated (see Table 2). The star-formation rates for Mrk 1456, and SDSS 21-00 are global Petrosian u-band SFRs corrected for internal extinction using the Balmer-line ratio and a Calzetti obscuration curve (Calzetti et al. 2000). For Mrk 1456 we adopt the Balmer-line ratio from König et al. (2006). For SDSS 21-00, we measure a Balmer-line ratio of 7.2 using the $H\alpha$ flux, corrected for absorption via Hopkins et al. (2003), and the $H\beta$ flux, with the absorption and emission components of the line deblended with two Gaussians. The u-band absolute magnitudes and star-formation rates are given in Table 2. We derive 3.1 ± 0.2 and $5.6 \pm 1.2 M_\odot \text{ yr}^{-1}$ for Mrk 1456 and SDSS 21-00, respectively, both in good agreement with the average SFRs for late-type spirals (Kennicutt 1983, 1998).

Table 2 lists several emission-line measured, and derived, properties for Mrk 1456 and SDSS 21-00. For Mrk 1456, we adopt the values from König et al. (2006) for emission-line fluxes and derived abundances. For SDSS 21-00, emission-line fluxes were measured by fitting Gaussians to the OIII, $H\beta$, NII, and $H\alpha$ emission-lines, while oxygen abundances were measured using the strong-line indices of $\frac{OIII[\lambda 5007]/H\beta}{NII[\lambda 6583]/H\beta}$ (O3N2),

²NASA Extragalactic Database

$\frac{NII[\lambda 6583]}{H\alpha}$ (N2) (Pettini & Pagel 2004) and R23 (Kobulnicky et al. 1999; McGaugh 1991). We find that the O3N2 and N2 derived abundances are in good agreement with each other. Assuming a solar abundance of 8.74 ± 0.08 from Holweger (2001), SDSS 21-00 has a metallicity near the solar value.

2.2. Green Bank Telescope Observations and Reduction

The observations of Mrk 1456 were made on 2006 August 27 with the Green Bank Telescope, a 100-m diameter single dish telescope with a FWHM beamwidth of $12.4'/f(\text{GHz})$. The L-band Gregorian receiver was used, which covers a frequency range of 1.15-1.73 GHz, giving a FWHM beamwidth of $9'$ with two linear polarizations. The gain on the L-band receiver is 2 K/Jy. The backend used was the GBT Spectrometer in the narrow bandwidth, high resolution mode. The spectrometer was set for a 12.5 MHz bandwidth, with 1 spectral window. 9-level sampling was employed to increase sensitivity and to improve the ability to excise Radio Frequency Interference (RFI). The raw spectral resolution was 0.38146 kHz over 32768 channels. We obtained 42 on/off pairs each with a 5 minute integration time resulting in a total integration time of 7 hours, including both signal and reference observations.

To reduce the data we (1) removed any Radio Frequency Interference (RFI) identified by eye in individual scans, (2) subtracted off a baseline, and (3) averaged the two polarizations to achieve the final spectrum. RFI usually presents itself as sharp spikes in the data. Each of the 84 scans was investigated, by eye, for any such spikes and, if found, the bad data were removed. During the RFI removal, two other problems were discovered in the data, including “Bad Lag”. “Bad Lag” refers to the incorrect scaling of the raw lags by the spectrometer (O’Neil, K. 2006)³. Each record, 2.5 seconds of data, where this “Bad Lag” occurred were removed from the scan. In addition, when the power spectrum of the data was analyzed, we found a sharp peak at a frequency corresponding to a standing wave on the antenna. The standing wave arises from light that is reflected back and forth between the reflector and the panel gaps on the telescope (Fisher et al. 2003). Due

to these standing waves, fourteen scans (140 minutes), were removed from the 1st polarization and eight scans (80 minutes) were removed from the 2nd polarization. Once the bad data were removed, a 3rd, 5th, or 7th order polynomial was fit to each scan and subtracted. After the subtraction of the baseline, each scan was then Hanning smoothed and then further smoothed with a 500 channel (45 km s^{-1}) boxcar filter. After smoothing the data, a weighted average of all of the scans in both polarizations was computed. Each scan is assigned a weight based on its antenna temperature, exposure time, and frequency resolution. Since an entire scan gets a single weight, the channels in a scan that were flagged for RFI removal have an incorrect weighting value for those channels. Because data in the flagged channels are removed but not down-weighted, they still contribute some noise to the average spectrum. However, the number of flagged channels for RFI removal in each scan is small enough that it does not cause any noticeable effects in the final averaging. The final spectrum is shown in Figure 1.

2.3. Arecibo Observations and Reduction

The data for SDSS 21-00 were taken with the 305m diameter Arecibo telescope on 2006 October 27 on the L-band wide receiver and the interim 50 MHz correlator. The correlator was configured for 9-level sampling in 2 linear polarizations with four boards. Two of the boards were centered on the 1420.4058 MHz line of neutral hydrogen while the other two boards were centered on the 1667.359 and 1720.530 MHz OH lines. Radio frequency interference was too strong at these higher frequencies to make use of the OH observations. For the HI observations, the center frequency was set to 1338.147 MHz, the expected emission frequency of the galaxy. One board was set up with a 25 MHz bandwidth while the other was set-up with a 6.25 MHz bandwidth. In both cases there were 2048 lags per board resulting in velocity resolutions of 2.9 and 0.7 km s^{-1} respectively, before Hanning smoothing.

Prior to the beginning of observations a test scan was taken on a blank sky position that showed emission from the 1350/1330 MHz FAA radar. Because of this emission, the radar blanker was used during the observations which reduces effective integration times by approximately a

³<http://wiki.gb.nrao.edu/bin/view/Software/ModificationRequest150306>

factor of 1/1.188. The observations of the source consist of 4 on/off observations of 5 minutes each. Each resulting on/off pair was combined, Hanning smoothed and a baseline was fit to the result and subtracted. The eight spectra – 4 on/off pairs with 2 polarizations each – were then averaged and an additional second order polynomial was subtracted from the resulting spectrum. An additional boxcar smoothing of 25 channels or 18.1 km s⁻¹ was applied to the spectrum. The final spectrum is shown in Figure 2.

2.4. Analysis

Two signals were detected in the GBT observations of Mrk 1456 (see Figure 1). Both signals show the typical double-horned profile as expected from an inclined disk galaxy. One signal is located at the frequency 1.35587±0.00003 GHz, and corresponds to a redshift of 0.04759±0.00002, which matches the SDSS redshift of Mrk 1456 (0.04757±0.00008) within the errors. The second signal, located at the frequency 1.3544±0.0001, corresponds to a redshift of 0.04873±0.00008, which matches the position and redshift of Mrk 1457 (SDSS redshift 0.04857±0.00009). Mrk 1457 is located about 2.3' south of Mrk 1456. Given the beamwidth of 9', we note that two other members, Mrk 1458 and SDSS J114711.09+522653.4, located at frequencies of 1.35517 GHz (14442 km s⁻¹) and 1.35574 GHz (14310 km s⁻¹) respectively, are also within the beam. Examination of the spectrum in Figure 1 shows that Mrk 1458 falls in the gap between Mrk 1456 and Mrk 1457, where the HI flux falls to zero. SDSS J114711.09+522653.4 falls in the middle of the signal of Mrk 1456. As there is no way to disentangle the two signals, there may be some contribution of HI from SDSS J114711.09+522653.4. However, SDSS J114711.09+522653.4 is an E/S0 galaxy that is 2.8' from Mrk 1456 (the beam center), so we expect the contribution to the HI flux to be small. The regular shape of the spectrum also indicates that this is the case.

The task Gmeasure in GBTIDL was used to measure the integrated flux, S(v)dv, in K · (km s⁻¹), the velocity width W, and systematic velocity of the galaxy profile. The rms noise in the data was taken as the error in the flux. The results of the analysis are shown in Table 3.

HI mass was determined from the data using

(Verschuur & Kellermann 1974)

$$\frac{M_{HI}}{M_{\odot}} = 2.4 \times 10^5 D^2 \int S(v)dv \quad (1)$$

where D is the luminosity distance in Mpc (see Table 2), and S(v)dv is the flux integrated over the line in Jy · (km s⁻¹)⁴. We include flux and distance errors on the HI mass measurement in Table 3.

We estimate the dynamical mass from

$$M_{dyn} = \frac{v_{rot}^2 * r_{HI}}{G} \quad (2)$$

where $r_{HI} = 1.5 * r_{opt}$ (Broeils & Rhee 1997), r_{opt} is the SDSS r-band Petrosian radius, and v_{rot} is the rotational velocity, estimated by $v_{rot} = \frac{W_{50}}{2 * \sin(i)}$, where i here is the optical inclination of the galaxy.

In addition to these basic HI properties of the galaxies, we calculate the HI gas mass fraction, defined as $f_{gas} = M_{HI}/M_{dyn}$, and the gas richness, M_{HI}/L_B . These values are also given in Table 3. All HI parameters were calculated using the HI line width at 50% of the peak.

3. Discussion

3.1. HI properties of Mrk 1456, SDSS J211701.26-002633.7, and Mrk 1457

We find that both Mrk 1456 and SDSS 21-00 have typical HI properties, ie. HI mass, gas richness, gas mass fraction, for galaxies with their given morphological types (Roberts & Haynes 1994; Salpeter & Hoffman 1996; Broeils & Rhee 1997). Mrk 1457, when compared to other Seyferts, lies at the high end of the normal range of HI masses ([0.2-9.0]x10⁹M_⊙) and appears to have an unusually large gas-mass fraction relative to the average f_{gas} of 0.009±0.002 for Seyferts (Haan et al. 2008).

Using the value of $M_{HI}^* = 6.3 \times 10^9$ from Zwaan et al. (2005), Mrk 1456 and Mrk 1457 are slightly sub- M_{HI}^* galaxies, while SDSS 21-00 is twice an M_{HI}^* galaxy. Mrk 1456 and SDSS 21-00 are representative of average Sb-Sc spiral galaxies with a fair amount of HI gas remaining, while having typical SFR rates of most spirals, indicative of

⁴S(v)dv is converted from K · (km s⁻¹) to Jy · (km s⁻¹) before M_{HI} is computed

an on-going SFR process and conversion of their neutral gas reservoir into stars.

3.2. Comparison with HI-detected DLAs

In the following, we discuss HI observations of known/candidate DLAs and sub-DLAs, namely, SBS 1543+593, NGC 4203, and the absorbers towards OI 363, PKS 0439-433, and PG 1216+069. The data are collected in Table 1. All values listed have been recalculated using the cosmology adopted in this paper, and all magnitudes listed are Johnson-Morgan-Cousins B-band magnitudes converted to the AB zeropoint system, except the magnitude of the OI 363 absorber which is a K-band magnitude.

Presently, only one bonafide DLA has been successfully detected in HI 21 cm emission (Bowen et al. 2001). SBS 1543+593, a $z=0.009$ dwarf spiral (Schulte-Ladbeck et al. 2004) is a quasar absorption line galaxy, first found through study of its emission lines (Martel & Osterbrock 1994; Reimers & Hagen 1998). SBS 1543+593 is a low surface brightness system that has been extensively studied in emission and absorption (Rosenberg et al. 2006; Bowen et al. 2001, 2005; Schulte-Ladbeck et al. 2005). It has HI properties consistent with other dwarf spirals (Roberts & Haynes 1994; Broeils & Rhee 1997; de Blok et al. 1996) including a low HI mass, a large M_{HI}/L_B , and a small gas mass fraction.

NGC 4203 was mapped in 21 cm (van Driel et al. 1988; Burstein & Krumm 1981) and exhibits a typical HI mass and f_{gas} for the average S0, but an atypically large gas richness (Roberts & Haynes 1994). The absorbers toward the QSOs OI 363 and PKS 0439-433 were undetected in 21 cm emission (Lane et al. 2000; Kanekar et al. 2001) but have 3σ upper limits to the HI mass. For the OI 363 absorber, it was not optically detected with the exception of two regions of patchy structure near the QSO OI 363, referred to as the “jet” and the “arm” (Turnshek et al. 2001). Although no optical counterpart has been found in conjunction with the $z=0.0063$ absorber towards PG 1216+069, a weak 21 cm emission signal was found at 3σ significance within $30''$ (3.8 kpc) of the QSO (Briggs & Barnes 2006).

Figure 3 provides a comparison of several of the galaxy properties listed in Tables 1 and 2. For

the morphological type, we assign a value to each type ranging from 0-E to 6-Irr, with intermediates taking half-integer values, ie. 2.5-Sab. For the $z=0.101$ galaxy associated with PKS 0439-433, Kanekar et al. (2001) report two upper limits to the HI mass, listed in Table 1 and in Figure 3, we plot the larger value for the upper limit to the HI mass and M_{HI}/L_B . The absorbers associated with OI 363 and PG 1216+069 are not included as no host galaxy has, as of yet, been clearly identified with the absorbing system. Five objects do not carry statistical weight, but are used to just highlight some broad trends and consistencies.

The morphologies of the DLAs/candidates in Fig. 3 consist of one dwarf, one S0 galaxy, and three giant late-type spirals. This diversity in galaxy types naturally accounts for some spread in the derived HI and optical properties shown in Fig. 3. With regards to their optical properties, SDSS 21-00 and Mrk 1456 fall right in the middle of the distribution of L^* , and M_{HI}/L_B^* values in the given sample. They do, however, exhibit one noteworthy property: they have the highest HI masses of the sample. Our observations of Mrk 1456 and SDSS 21-00 have added two candidate DLA galaxies with morphologies and luminosities of giant late-type spirals. Thus they are most directly comparable to the galaxy toward PKS 0439-433, also a late-type giant spiral. The PKS galaxy is an Sab class sub-DLA with an HI column just below the DLA limit, and an impact parameter that is just outside its stellar disk. Given that HI column densities are higher at lower radii and in later morphological subtypes, we expect that future observations on the QSO sightlines of Mrk 1456 and SDSS 21-00 might reveal HI column densities larger than the DLA limit, as both are later subtypes than the PKS galaxy and both have sightlines to their QSOs that lie inside their stellar disks. The properties of Mrk 1456 and SDSS 21-00 agree within the distributions of expected optical properties of $z=0$ DLAs.

Rosenberg et al. (2006) found that SBS 1543+593 is in a small galaxy group with three other companions, a disk galaxy and two dwarfs, all of which are of low luminosity. All three companions are gas rich systems, with low HI mass ($< 10^9 M_\odot$), and average gas content for disk and late-type dwarf galaxies (see Rosenberg et al. 2006, Table 2). This group, and other small groups like it,

are likely to be fairly common and important in the contribution to the DLA population. Furthermore, if young, gas-rich galaxy groups are more prevalent at higher redshifts, then these systems might be important to the DLA cross-section. From a search using the NASA/IPAC extragalactic database (NED), none of the other DLAs that have been observed in 21 cm have associated groups, but faint dwarfs could have been missed.

Merchán & Zandivarez (2005) completed a sample of galaxy groups in the DR3 of the Sloan Digital Sky Survey (SDSS). Mrk 1456 is in one such group, with four other members. Mrk 1457 is one such member. All other galaxies in the group are contained within the beam of the GBT, centered on Mrk 1456, but Mrk 1457 was the only other member to be detected in HI 21 cm emission. Merchán & Zandivarez (2005) also show that SDSS 21-00 is in a group, consisting of seven other members. Table 4 lists a few global properties of the group, ie. the group coordinates, group systematic velocity, group velocity width, virial mass and radius of the group, as calculated by Merchán & Zandivarez (2005) and Table 5 lists each group’s members and their properties. As both galaxies are situated in groups, the question of misidentification of the DLA host galaxy becomes an issue. Traditionally, identifying DLA hosts has proven difficult since either no obvious galaxy is visible or identifying the correct host in a group is difficult as the galaxy giving rise to the line may not be the brightest or closest galaxy to the QSO. This is not an issue with Mrk 1456 or SDSS 21-00. For both systems, the QSO lies within the stellar disk of the galaxy, and in both groups, the closest companion outside the named galaxy here lies more than 120 kpc from the QSO.

Without HI observations of the galaxies in these groups, it is hard to determine the richness of the group and the environment these galaxies live in. We use u-r color and morphological type as a rough indicator of the gas content of the other galaxies in these groups. The reliability, however, of using optical properties as a predictor of gas content is uncertain as HI-selected galaxies differ more in their optical properties than optically-selected ones, the exception being the most blue galaxies, as they have retained most of their primordial gas. Figure 5 shows how galaxies of dif-

ferent morphologies segregate in color and concentration. We plot the galaxies from Park & Choi (2005) overlaid with the Mrk 1456 group (black circles) and the SDSS 21-00 group (black diamonds). The galaxies in the Mrk 1456 group, with the exception of Mrk 1456, fall in the region of the diagram occupied by early types. The galaxies in the SDSS 21-00 galaxy group, on the other hand, are predominantly Sb-Sc morphological types with only two E/S0 galaxies. Kannappan (2004) showed that there is a relationship between u-r color and gas richness. Galaxies with $u-r < 1.5$ are gas-rich, $1.5 < u-r < 2.5$ are intermediate in gas richness, and those with $u-r > 2.5$ are generally gas-poor. The u-r colors of the galaxies in the two galaxy groups are listed in Table 5. These results indicate that both the Mrk 1456 and SDSS 21-00 galaxy groups are intermediate in their gas-richness.

The total HI mass of all 4 galaxies detected in the SBS 1543+593 galaxy group adds up to $< 3 \times 10^9 M_{\odot}$. With two of four galaxies detected in the Mrk 1456 group, its HI content is already much larger, $\sim 12 \times 10^9 M_{\odot}$. The single galaxy detected in the SDSS 21-00 galaxy group has an HI mass of $\approx 14 \times 10^9 M_{\odot}$, much larger than the entire SBS 1543+593 galaxy group.

3.3. Comparison with HI-detected galaxies

West (2005) used SDSS to identify optical counterparts of HI-selected galaxies from HIPASS and found that HI-selection yields a high fraction of late-type galaxies. For HI-selected spirals, West et al. (2008) give the following median properties: $M_{HI}/L_B = 0.5$, $M_{HI} = M_{HI}^*$, and $L_B = 0.6 L_B^*$. Our Ca II absorbing galaxies appear to have properties that are comparable to those of HI-selected galaxies.

Rosenberg & Schneider (2003) and Ryan-Weber et al. (2003) also looked at HI-selected galaxies, and focused more specifically on the question of how these contribute to the DLA cross-section. Rosenberg & Schneider (2003) find a tight correlation between the expected DLA cross-section and the HI mass. Their equation 3 predicts the following DLA cross-sections for Mrk 1456 and SDSS 21-00: 853.7 kpc^2 and 2058.4 kpc^2 . Using these sizes to estimate the average column density for the galaxies, we find for Mrk 1456,

$N_{HI} = 8.23 \times 10^{20} \text{ cm}^{-2}$, and for SDSS 21-00, $N_{HI} = 8.25 \times 10^{20} \text{ cm}^{-2}$. Rosenberg & Salzer (in prep.) looked at the predicted optical properties for $z=0$ DLAs from an HI-selected sample and find that the most common morphological type is spiral (45%) and that 50% of the DLAs should have an $M_{HI}/L_B > 0.77$ (2 of the 6 galaxies from the Rosenberg & Salzer (in prep.) sample are from this sample). Ryan-Weber et al. (2003) also find that gas-rich, late-type spirals contribute most to the DLA cross-section.

Figure 4 shows the HI mass contribution to dN/dz , the number of expected systems per unit redshift, for $z \sim 0$, for a sample of HI-selected galaxies with an HI column larger than the DLA limit from the Arecibo Dual-Beam Survey (ADBS, see Rosenberg & Schneider (2003) for details). The figure shows that 50% of the cross-sectional area is from galaxies with HI masses between 2.9×10^8 and 3.5×10^9 . The red-hatched histogram overlaid on top is the HI mass distribution of the objects listed in Tables 1 and 2, with the exception of the OI 363 absorber. The right hand axis lists the values for this histogram, N , the number of galaxies. One might expect the HI mass distribution of DLAs in general to follow the same HI mass distribution of HI-selected galaxies expected to be DLAs. It should be noted that the two galaxy/QSO pairs we add here were not selected using the traditional selection method for quasar absorption line systems, ie. through UV absorption lines. Thus, they introduce some bias in the HI mass distribution as they are giant spirals optically-selected from SDSS with quasars projected within their stellar disks. However, even with this caveat and low statistics, it appears the HI mass distribution of the (candidate) DLAs mimics the distribution of HI-selected galaxies expected to be DLAs.

Zwaan et al. (2005) looked at an optically-selected sample of the local galaxy population ($z \sim 0$), mapped in 21 cm emission, in order to connect them to the low-redshift ($z < 1$) DLA population and calculated expected probability distribution functions of different properties for the low-redshift DLAs. They find that, for expected DLA systems, most will be late-type, with a median impact parameter of $8.0 \text{ kpc}_{-5.3}^{+10.8}$, median $\log M_{HI}$ of $9.3_{-0.7}^{+0.5}$, and median $M_B = -17.98_{-2.0}^{+2.7}$. Mrk 1456 and SDSS 21-00 are indeed late-types within the range for the expected impact param-

eter and have values for HI mass and absolute magnitude that lie close to the expected values, on the high end.

4. Conclusion

We report on the HI 21 cm emission observations of two galaxies, Mrk 1456 and SDSS J211701.26-002633.7. Both are average disk galaxies and candidate DLAs, based on the strengths of their Ca II K EW's and their low impact parameters to the QSO. In terms of their HI properties, both galaxies have typical HI properties for their morphological types with $M_{HI} \sim M_{HI}^*$, average gas richness, and gas mass fractions that are representative of disk galaxies.

These data add to the total number of strong candidate DLAs with HI observations, in the local Universe. Compared with other HI-detected DLAs, Mrk 1456 and SDSS 21-00 are similar in most respects, with comparatively higher HI masses. When compared to the expected properties of $z=0$ DLAs from HI-detected galaxies, we find that Mrk 1456 and SDSS 21-00 fall within range of the expected HI mass distribution, median impact parameter, and absolute magnitudes for local DLAs. We also find that both Mrk 1456 and SDSS 21-00 reside in groups, adding two DLAs in gas-rich groups to the known population. This may indicate a common phenomenon with regards to the environment of DLAs.

In spite of many years of observational effort, associated galaxies have only been identified in a very small fraction of known DLA systems. Therefore, the nature of the evolving DLA galaxy population has continued to be under investigation, both observationally and theoretically. Historically, two very different scenarios were developed to explain what kind of galaxies produce DLAs. In the explanation put forth by Wolfe et al. (1986), DLAs are associated with massive spiral galaxies. In the model proposed by Haehnelt et al. (1998), DLAs instead arise in low-mass dwarf galaxies.

The numerical and semi-analytical galaxy formation simulations presented over the last decade have modified our view of DLAs. Current models suggest that the median properties of DLA galaxies and their range evolve as a function of cosmic time. In this scenario, dwarfs make up most of the DLA cross-section at high redshifts, with massive

disk galaxies contributing more as the Universe evolves. Johansson & Efstathiou (2006) find that higher mass systems make an increasing contribution to the DLA population as redshift decreases. Specifically, Johansson & Efstathiou (2006) predict a median DLA Hydrogen mass of $M_{HI} = 2 \times 10^9 M_{\odot}$ at $z=0$; in good agreement with the results for HI-selected galaxies (Zwaan et al. 2005), and what we find here (cf. Fig. 4). Thus, although Mrk 1456 and SDSS 21-00 are case studies of bright QSOs seen through the disks of nearby spiral galaxies, we do not conclude that they support the original Wolfe et al. (1986) picture. Rather, we interpret our results to be compatible with the current theoretical models, as galaxies contributing to the fraction of disk galaxies that make up the DLA cross-section at low redshift. We conclude that our result further strengthens the picture that the local galaxy population, in its variety of gas rich galaxy types that randomly intercept QSO sightlines, can explain the properties of the low-redshift DLAs.

We are grateful to Toney Minter, Karen O’Neil, and Jay Lockman at the GBT for their help in the observations and reduction of the data. The National Radio Astronomy Observatory is a facility of the National Science Foundation operated under cooperative agreement by Associated Universities, Inc.

We thank Chris Salter and Tapasi Ghosh for handling the Arecibo observations. The Arecibo Observatory is part of the National Astronomy and Ionosphere Center, which is operated by Cornell University under a cooperative agreement with the National Science Foundation.

We wish to thank Andrew West for making details of his Ph.D thesis available to us.

We also made use of data obtained at the Gemini Observatory, which is operated by the Association of Universities for Research in Astronomy, Inc., under a cooperative agreement with the NSF on behalf of the Gemini partnership: the National Science Foundation (United States), the Science and Technology Facilities Council (United Kingdom), the National Research Council (Canada), CONICYT (Chile), the Australian Research Council (Australia), Ministrio da Ciencia e Tecnologia (Brazil) and SECYT (Argentina).

Funding for the SDSS and SDSS-II has been

provided by the Alfred P. Sloan Foundation, the Participating Institutions, the National Science Foundation, the U.S. Department of Energy, the National Aeronautics and Space Administration, the Japanese Monbukagakusho, the Max Planck Society, and the Higher Education Funding Council for England. The SDSS Web Site is <http://www.sdss.org/>. The SDSS is managed by the Astrophysical Research Consortium for the Participating Institutions. The Participating Institutions are the American Museum of Natural History, Astrophysical Institute Potsdam, University of Basel, University of Cambridge, Case Western Reserve University, University of Chicago, Drexel University, Fermilab, the Institute for Advanced Study, the Japan Participation Group, Johns Hopkins University, the Joint Institute for Nuclear Astrophysics, the Kavli Institute for Particle Astrophysics and Cosmology, the Korean Scientist Group, the Chinese Academy of Sciences (LAMOST), Los Alamos National Laboratory, the Max-Planck-Institute for Astronomy (MPIA), the Max-Planck-Institute for Astrophysics (MPA), New Mexico State University, Ohio State University, University of Pittsburgh, University of Portsmouth, Princeton University, the United States Naval Observatory, and the University of Washington.

This research has made use of NASA’s Astrophysics Data System and of the NASA/IPAC Extragalactic Database (NED) which is operated by the Jet Propulsion Laboratory, California Institute of Technology, under contract with the National Aeronautics and Space Administration.

REFERENCES

- Blanton, M. R., & Roweis, S. 2007, *AJ*, 133, 734
- Boissier, S., Péroux, C., & Pettini, M. 2003, *MNRAS*, 338, 131
- Bowen, D. V., Huchtmeier, W., Brinks, E., Tripp, T. M., & Jenkins, E. B. 2001, *A&A*, 372, 820
- Bowen, D. V., Tripp, T. M., & Jenkins, E. B. 2001, *AJ*, 121, 1456
- Bowen, D. V., Jenkins, E. B., Pettini, M., & Tripp, T. M. 2005, *ApJ*, 635, 880
- Briggs, F. H., & Barnes, D. G. 2006, *ApJ*, 640, L127

- Broeils, A. H., & Rhee, M.-H. 1997, *A&A*, 324, 877
- Burstein, D., & Krumm, N. 1981, *ApJ*, 250, 517
- Calzetti, D., Armus, L., Bohlin, R. C., Kinney, A. L., Koornneef, J., & Storchi-Bergmann, T. 2000, *ApJ*, 533, 682
- Cardelli, J. A., Clayton, G. C., & Mathis, J. S. 1989, *ApJ*, 345, 245
- Cayatte, V., Kotanyi, C., Balkowski, C., & van Gorkom, J. H. 1994, *AJ*, 107, 1003
- Chen, H.-W., & Lanzetta, K. M. 2003, *ApJ*, 597, 706
- Chen, H.-W., Kennicutt, R. C., Jr., & Rauch, M. 2005, *ApJ*, 620, 703
- Chengalur, J. N., & Kanekar, N. 2002, *A&A*, 388, 383
- Christensen, L., Wisotzki, L., Roth, M. M., Sánchez, S. F., Kelz, A., & Jahnke, K. 2007, *A&A*, 468, 587
- de Blok, W. J. G., McGaugh, S. S., & van der Hulst, J. M. 1996, *MNRAS*, 283, 18
- Fisher, J. R., Norrod, R. D., & Balser, D. S. 2003, "Investigation of Spectral Baseline Properties of the Green Bank Telescope"
- Frei, Z., & Gunn, J. E. 1994, *AJ*, 108, 1476
- Gardner, J. P., Katz, N., Hernquist, L., & Weinberg, D. H. 2001, *ApJ*, 559, 131
- Haan, S., Schinnerer, E., Mundell, C. G., García-Burillo, S., & Combes, F. 2008, *AJ*, 135, 232
- Haehnelt, M. G., Steinmetz, M., & Rauch, M. 1998, *ApJ*, 495, 647
- Helou, G., Khan, I. R., Malek, L., & Boehmer, L. 1988, *ApJS*, 68, 151
- Holmberg, J., Flynn, C., & Portinari, L. 2006, *MNRAS*, 367, 449
- Holweger, H. 2001, Joint SOHO/ACE workshop "Solar and Galactic Composition", 598, 23
- Hopkins, A. M., et al. 2003, *ApJ*, 599, 971
- Johansson, P. H., & Efstathiou, G. 2006, *MNRAS*, 371, 1519
- Kannappan, S. J. 2004, *ApJ*, 611, L89
- Kanekar, N., Chengalur, J. N., Subrahmanyan, R., & Petitjean, P. 2001, *A&A*, 367, 46
- Kanekar, N., & Chengalur, J. N. 2005, *A&A*, 429, L51
- Kennicutt, R. C., Jr. 1992, *ApJS*, 79, 255
- Kennicutt, R. C., Jr. 1983, *ApJ*, 272, 54
- Kennicutt, R. C., Jr. 1998, *ARA&A*, 36, 189
- Kobulnicky, H. A., Kennicutt, R. C., Jr., & Pizagno, J. L. 1999, *ApJ*, 514, 544
- König, B., Schulte-Ladbeck, R. E., & Cherinka, B. 2006, *AJ*, 132, 1844
- Lane, W. M., Briggs, F. H., & Smette, A. 2000, *ApJ*, 532, 146
- Le Brun, V., Bergeron, J., Boisse, P., & Deharveng, J. M. 1997, *A&A*, 321, 733
- Loveday, J. 2000, *MNRAS*, 312, 557
- Marinoni, C., Monaco, P., Giuricin, G., & Costantini, B. 1999, *ApJ*, 521, 50
- Martel, A., & Osterbrock, D. E. 1994, *AJ*, 107, 1283
- Merchán, M. E., & Zandivarez, A. 2005, *ApJ*, 630, 759
- McGaugh, S. S. 1991, *ApJ*, 380, 140
- Miller, E. D., Knezek, P. M., & Bregman, J. N. 1999, *ApJ*, 510, L95
- Nagamine, K., Wolfe, A. M., Hernquist, L., & Springel, V. 2007, *ApJ*, 660, 945
- Nestor, D. B., Pettini, M., Hewett, P. C., Rao, S., & Wild, V. 2008, *MNRAS*, 1176
- Okoshi, K., & Nagashima, M. 2005, *ApJ*, 623, 99
- Park, C., & Choi, Y.-Y. 2005, *ApJ*, 635, L29
- Petitjean, P., Theodore, B., Smette, A., & Lespine, Y. 1996, *A&A*, 313, L25

- Pettini, M., & Pagel, B. E. J. 2004, *MNRAS*, 348, L59
- Poggianti, B. M. 1997, *A&AS*, 122, 399
- Prochaska, J. X., & Wolfe, A. M. 1997, *ApJ*, 487, 73
- Rao, S. M., & Turnshek, D. A. 1998, *ApJ*, 500, L115
- Rao, S. M., Nestor, D. B., Turnshek, D. A., Lane, W. M., Monier, E. M., & Bergeron, J. 2003, *ApJ*, 595, 94
- Reimers, D., & Hagen, H.-J. 1998, *A&A*, 329, L25
- Roberts, M. S., & Haynes, M. P. 1994, *ARA&A*, 32, 115
- Rosenberg, J. L., & Schneider, S. E. 2003, *ApJ*, 585, 256
- Rosenberg, J. L., Bowen, D. V., Tripp, T. M., & Brinks, E. 2006, *AJ*, 132, 478
- Ryan-Weber, E. V., Webster, R. L., & Staveley-Smith, L. 2003, *MNRAS*, 343, 1195
- Salpeter, E. E., & Hoffman, G. L. 1996, *ApJ*, 465, 595
- Schlegel, D. J., Finkbeiner, D. P., & Davis, M. 1998, *ApJ*, 500, 525
- Schneider, D. P., et al. 2007, *AJ*, 134, 102
- Schulte-Ladbeck, R. E., Rao, S. M., Drozdovsky, I. O., Turnshek, D. A., Nestor, D. B., & Pettini, M. 2004, *ApJ*, 600, 613
- Schulte-Ladbeck, R. E., König, B., Miller, C. J., Hopkins, A. M., Drozdovsky, I. O., Turnshek, D. A., & Hopp, U. 2005, *ApJ*, 625, L79
- Shimasaku, K., et al. 2001, *AJ*, 122, 1238
- Smith, J. A., et al. 2002, *AJ*, 123, 2121
- Strauss, M. A., et al. 2002, *AJ*, 124, 1810
- Tripp, T. M., Jenkins, E. B., Bowen, D. V., Prochaska, J. X., Aracil, B., & Ganguly, R. 2005, *ApJ*, 619, 714
- Tully, R. B., Pierce, M. J., Huang, J.-S., Saunders, W., Verheijen, M. A. W., & Witchalls, P. L. 1998, *AJ*, 115, 2264
- Turnshek, D. A., Rao, S., Nestor, D., Lane, W., Monier, E., Bergeron, J., & Smette, A. 2001, *ApJ*, 553, 288
- van Driel, W., van Woerden, H., Schwarz, U. J., & Gallagher, J. S., III 1988, *A&A*, 191, 201
- Verschuur, G. L., & Kellermann, K. I. 1974, New York, Springer-Verlag, 1974.
- Wild, V., & Hewett, P. C. 2005, *MNRAS*, 361, L30
- Wild, V., Hewett, P. C., & Pettini, M. 2006, *MNRAS*, 367, 211
- West, A. A. 2005, Ph.D. Thesis
- West, A. A., Garcia-Appadoo, D. A., Dalcanton, J. J., Disney, M. J., Rockosi, C. M., Ivezić, Ž, Bentz, M. C., & Brinkmann, J. 2008, *AJ*, submitted
- Wolfe, A. M., Turnshek, D. A., Smith, H. E., & Cohen, R. D. 1986, *ApJS*, 61, 249
- Wolfe, A. M., Gawiser, E., & Prochaska, J. X. 2005, *ARA&A*, 43, 861
- Zwaan, M. A., van der Hulst, J. M., Briggs, F. H., Verheijen, M. A. W., & Ryan-Weber, E. V. 2005, *MNRAS*, 364, 1467

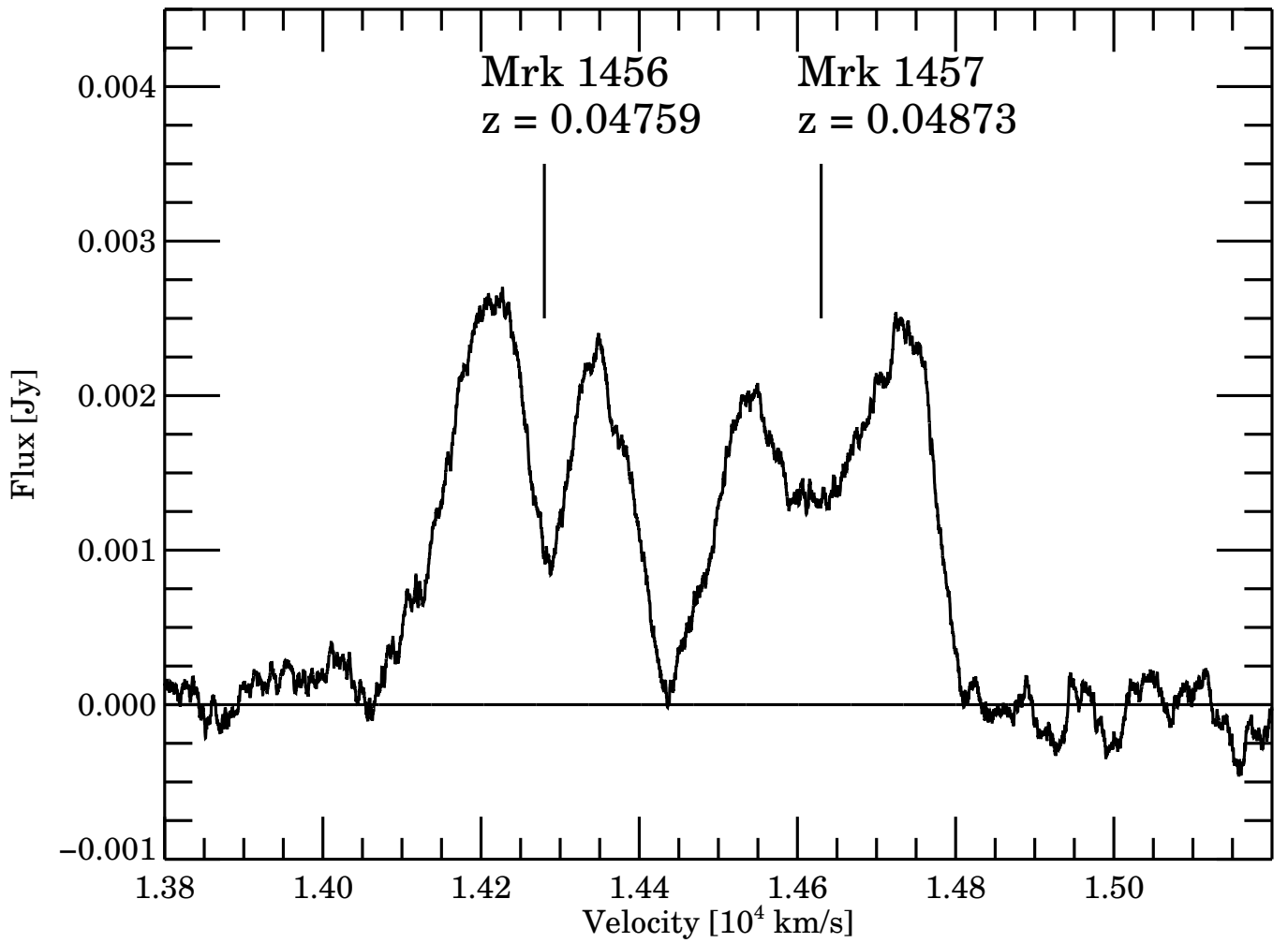


Fig. 1.— HI 21 cm spectrum from GBT showing Mrk 1456 and Mrk 1457

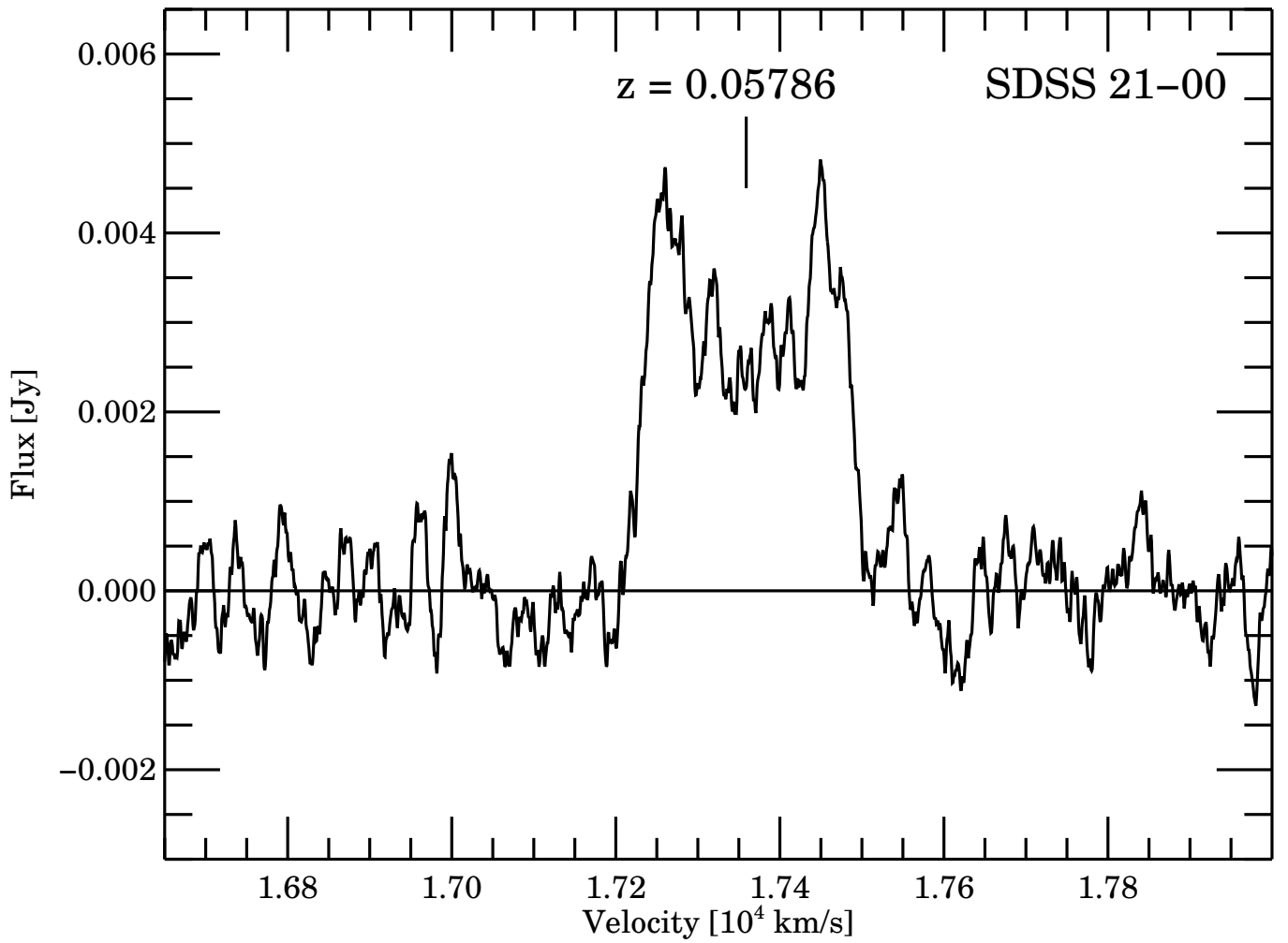


Fig. 2.— HI 21 cm spectrum from Arecibo showing SDSS J211701.26-002633.7

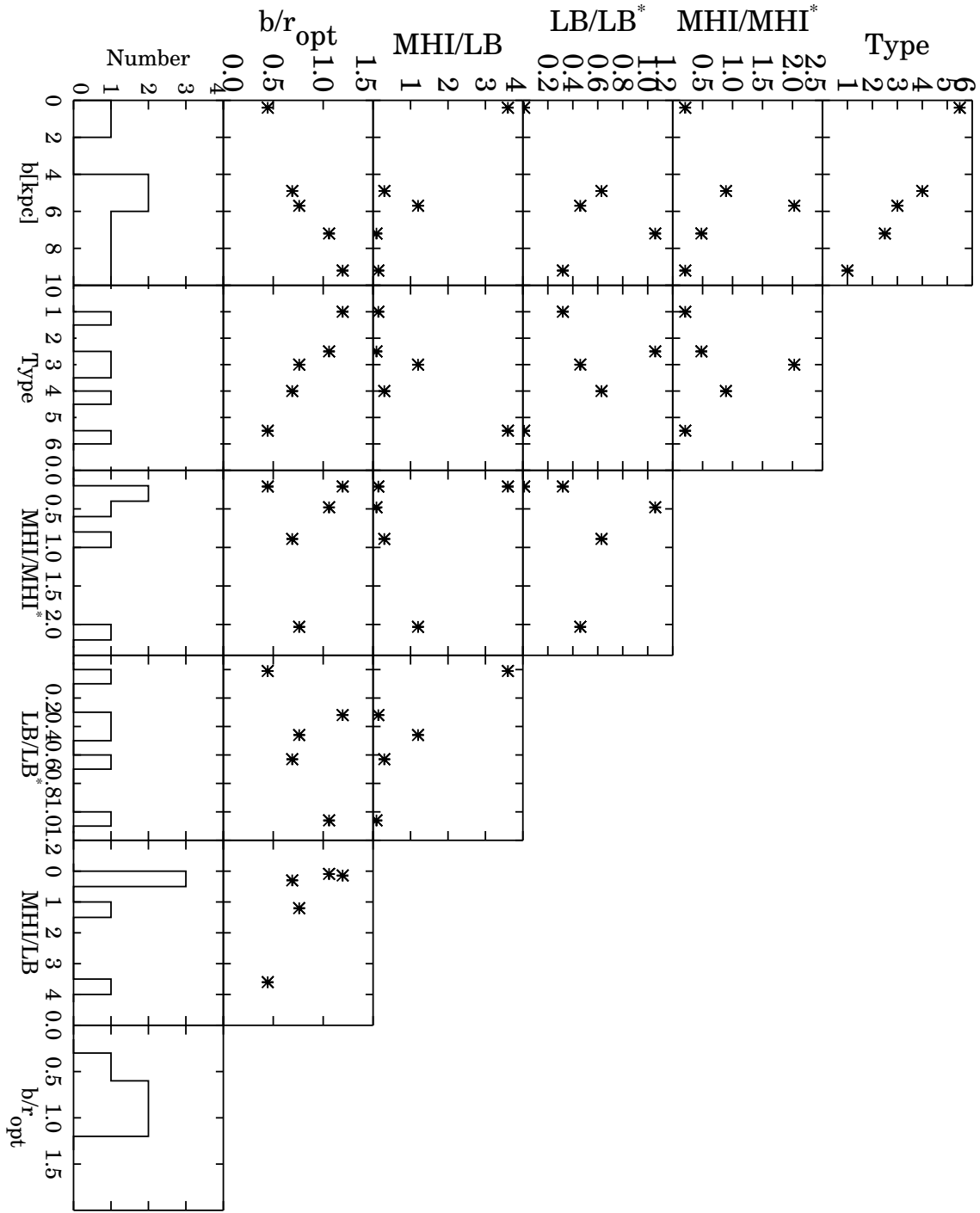


Fig. 3.— Histograms and plots of impact parameter, morphological type, M_{HI} , L_B , M_{HI}/L_B , and ratio of impact parameter to optical radius of the HI DLAs sample. The morphological type is represented with numbers from 0-6 for types E-Irr, respectively. M_{HI} is in units of M_{HI}^* and L_B is in units of L_B^* . The absorbers associated with OI 363 and PG 1216+069 are omitted from the diagram.

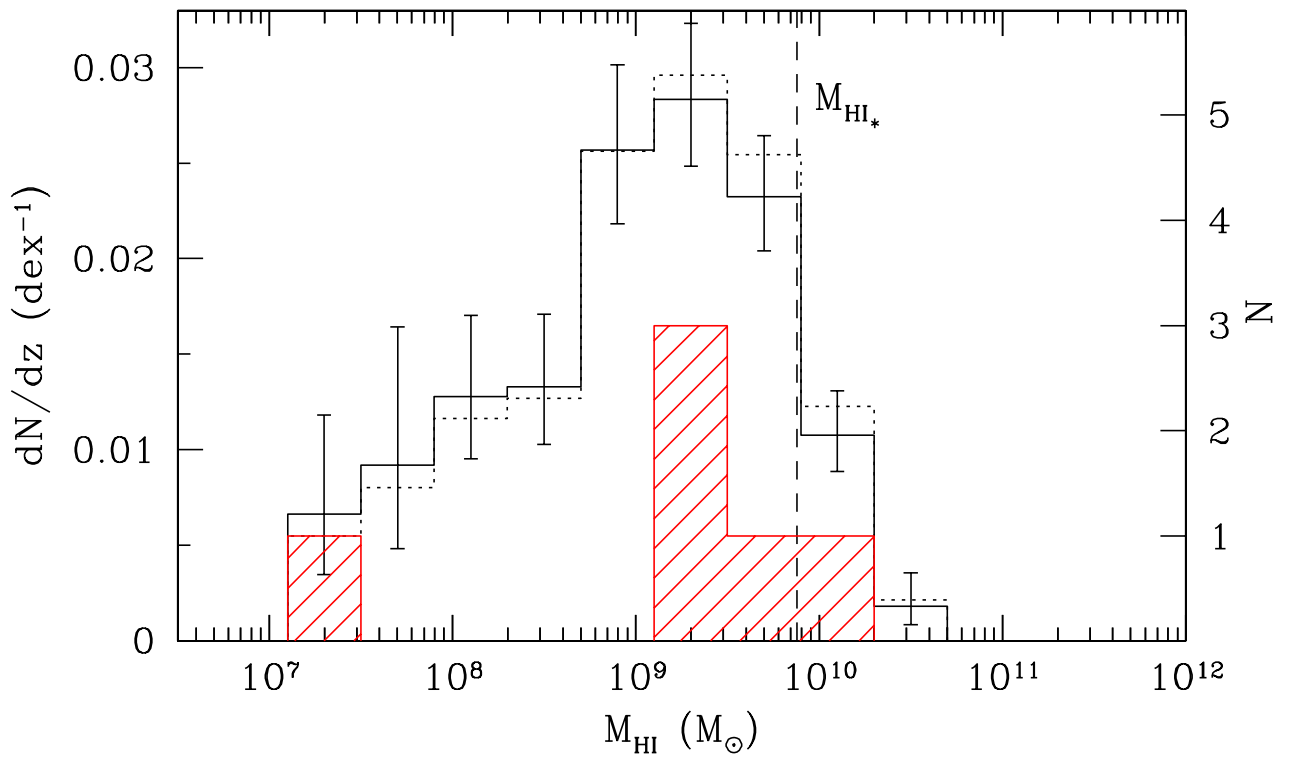


Fig. 4.— dN/dz as a function of HI mass. The open solid and dashed histograms show the distribution for a HI-selected sample of galaxies, representative of $z=0$ DLAs, from Rosenberg & Schneider (2003). The red hatched histogram shows the HI masses for the DLA systems listed in Tables 1 and 3. The right-hand axis shows the number of galaxies. The dashed line indicates M_{HI^*} .

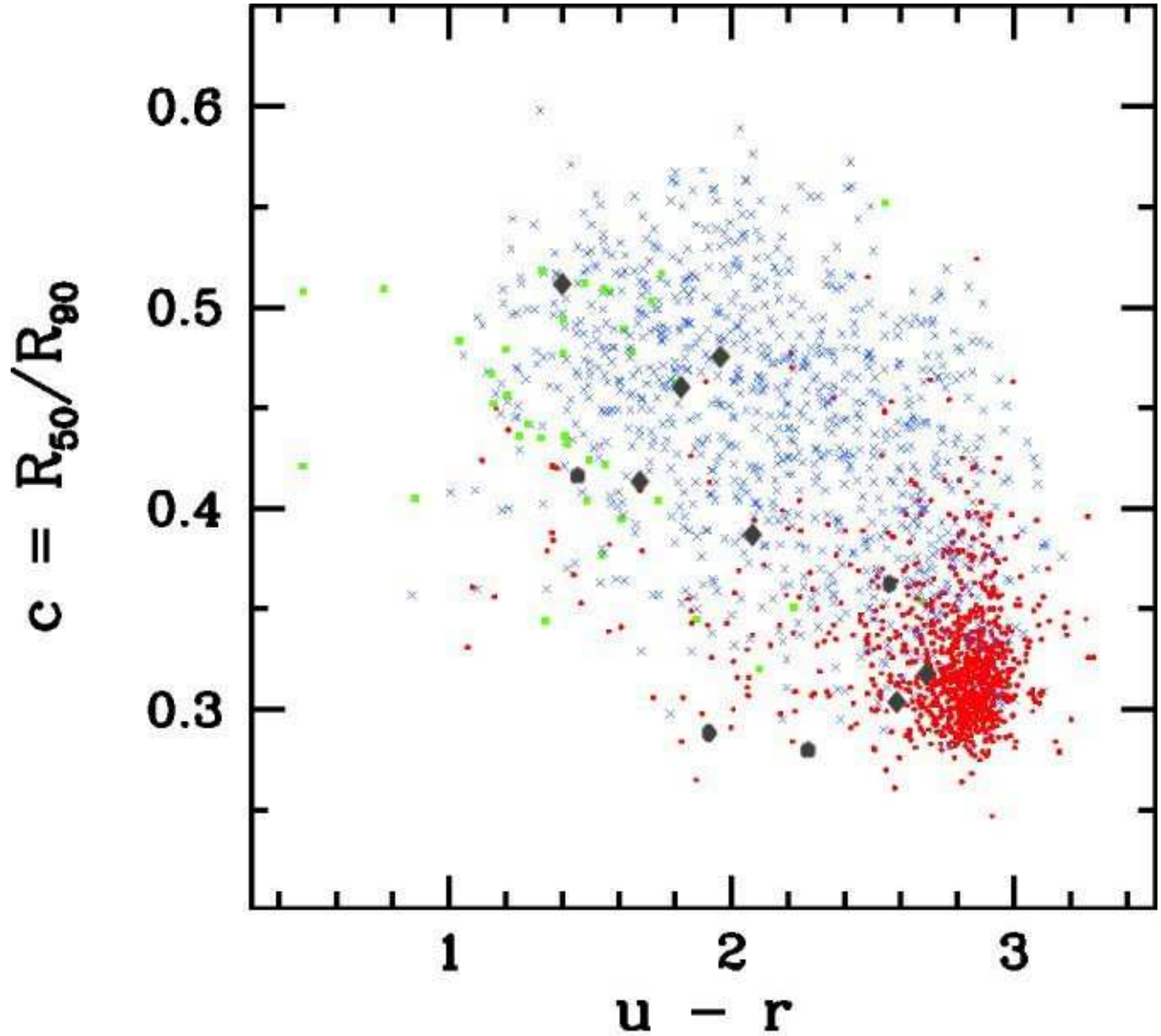


Fig. 5.— Galaxy concentration index versus optical color. The red circles show early type galaxies, green squares show intermediate types, and blue circles show late types from Park & Choi (2005). The black dots are the Mrk 1456 galaxy group members and the black diamonds are the SDSS 21-00 group members. Most members from the Mrk 1456 group tend to be early-types, while most from the SDSS 21-00 group tend to be late-types, suggesting the latter group is overall more gas-rich than the former.

Table 1: Optical and HI properties of Known/Candidate DLA Galaxies

Property	SBS 1543+593	NGC 4203	'Galaxy'	"Jet" ^a	"Arm"	–
type ^b	Sdm	SO	Sab	LSB	LSB	–
z	0.009±0.001	0.0036±0.00001	0.101±0.001	0.09118±0.00001	0.09118±0.00001	0.00632±0.00002
D_L [Mpc]	38.3±4.3	15.25±0.4	460.0±4.6	412.46±0.04	412.46±0.04	26.84±0.08
QSO	HS 1543+5921	Ton 1408	PKS 0439-433	OI 363	OI 363	PG 1216+069
z_{QSO}	0.807±0.002	0.6156±0.0002	0.593±0.003	0.631±0.002	0.631±0.002	0.3313±0.0003
b[^o]	2.4	126	3.9	<2	<2	<30
b[kpc]	0.4	9.2	7.2	<3.4	<3.4	<3.9
r[^o] ^c	4.8	105	3.7	4	4	–
r[kpc] ^c	0.9	7.7	6.8	6.7	6.7	–
axis ratio b/a	0.777	0.880	0.556	–	–	–
i^d [^o]	40	29	58	–	–	–
$M_B^{k,f,i,e}$	-16.1±0.2	-19.65±0.01	-20.96±0.08	-14.72 ^f	-15.12 ^f	–
L_B [$10^{10} L_\odot$]	0.04±0.01	0.96±0.02	3.2±0.2	0.01	0.02	–
L_B^*	0.01	0.32	1.06±0.07	0.0001	0.0002	–
$SFR[M_\odot yr^{-1}]^g$	0.006	0.16	–	–	–	–
$W_{50}[kms^{-1}]$	75	243	–	–	–	–
$M_{HI}[10^9 M_\odot]$	1.3±0.1	1.3	<(2.15-3.02)	<3	<3	(0.006-0.017)
M_{HI}^*	0.21	0.21	<0.34-0.48	<0.48	<0.48	(0.001-0.002)
$M_{dyn}[10^{11} M_\odot]$	0.07	1.2	–	–	–	–
$\frac{M_{HI}}{L_B}$	3.6±0.9	0.14±0.01	<(0.06-0.09)	<30	<20	–
$\frac{M_{HI}}{M_{dyn}}$	0.19	0.01	–	–	–	–
$\log N_{HI}[cm^{-2}]^h$	20.42±0.04	20.34	19.85±0.10	21.18±0.06	21.18±0.06	19.32±0.03
Refs ⁱ	1,2,3,4	5,6	7,8,9,10	11,12,13	11,12,13	14,15,16

^a Cherinka, König, & Schulte-Ladbeck attempted detection of H α of the "jet" with the GMOS-N IFU, but none was found, 2005, unpublished

^b morphological classification

^c radius estimates for: SBS 1543 & NGC 4203 - from diameter of 25th B-band isophote; PKS 0439-433 galaxy - radius towards QSO, measured from V band image; OI 363 - using K band estimate ⁸

^d SBS 1543 - HI incl. measured from rotation curve; NGC 4203 - HI inclination of inner disk; PKS 0439-433 galaxy - optical incl. from K-band

^e absolute B-band magnitude: superscripts k, f, and i denote the magnitude is k-corrected, foreground extinction corrected, and internal extinction corrected via Tully et al. (1998), respectively

^f K-band magnitudes, not internal extinction corrected, converted to luminosity using Loveday (2000) solar value

^g SBS 1543 SFR - total H_α star-formation rate from Schulte-Ladbeck et al. (2004); NGC 4203 SFR - FIR star-formation rate calculated with 60 and 100 μm flux densities available from the Infrared Astronomical Satellite (IRAS) along with equations from Helou et al. (1988) and Hopkins et al. (2003)

^h N_{HI} source: SBS 1543 - Ly- α line; NGC 4203 - X-ray absorption; PKS 0439-433 galaxy - Ly- α line; Jet and Arm near OI 363 - Ly- α line; Unknown galaxy with PG 1216+069 - HI 21cm emission

ⁱ 1-Bowen et al. (2001); 2-Rosenberg et al. (2006); 3-Schulte-Ladbeck et al. (2004); 4-Chengalur & Kanekar (2002);

5-Miller et al. (1999); 6-van Driel et al. (1988); 7-Kanekar et al. (2001); 8-Petitjean et al. (1996);

9-Chen & Lanzetta (2003); 10-Chen et al. (2005); 11-Lane et al. (2000); 12-Turnshek et al. (2001); 13-Rao & Turnshek (1998);

14-Briggs & Barnes (2006); 15-Tripp et al. (2005); 16-Kanekar & Chengalur (2005)

Table 2: Optical Properties of Mrk 1456 and SDSS 21-00

Property	Mrk 1456	SDSS 21-00
Type	Sc	Sb
z	0.04757 ± 0.00008	0.05792 ± 0.00009
D_L [Mpc]	208.5 ± 0.3	255.8 ± 0.4
QSO	SDSS J114719.89+522923.1	SDSS J211701.31-0026.38.8
z_{QSO}	1.99	1.14
b["]	5.3	5.1
b[kpc]	4.9	5.7
r["]	7.7	6.7
r[kpc]	7.1	7.5
axis ratio b/a	0.724	0.638
i[°]	45	52
$M_r^{k,f}$	-20.58 ± 0.01	-20.14 ± 0.01
$M_u^{k,f}$	-19.14 ± 0.02	-18.55 ± 0.04
$SFR_u [M_\odot yr^{-1}]$	3.1 ± 0.2	5.6 ± 1.2
$M_B^{k,f,i}$	-20.40 ± 0.09^a	-20.07 ± 0.09
$L_B [10^{10} L_\odot]^b$	1.92 ± 0.16	1.41 ± 0.12
L_B^*	0.63 ± 0.05	0.46 ± 0.04
REW(CaII)	1.24 ± 0.15	1.1 ± 0.2
$H\alpha [10^{-16} \text{ergs cm}^{-2} \text{s}^{-1}]$	65.65 ± 0.3	20.3 ± 0.2
$L_{H\alpha} [10^{40} \text{ergs s}^{-1}]^c$	8.64 ± 1.69	13.8 ± 0.2
$N_{HI d} [10^{22} \text{cm}^{-2}]^d$	1.8	3.0
$H\beta [10^{-16} \text{ergs cm}^{-2} \text{s}^{-1}]$	15.15 ± 0.2	2.8 ± 0.2
$[NII]\lambda 6550 [10^{-16} \text{ergs cm}^{-2} \text{s}^{-1}]$	6.8 ± 0.2	2.09 ± 0.14
$[NII]\lambda 6585 [10^{-16} \text{ergs cm}^{-2} \text{s}^{-1}]$	19.40 ± 0.3	5.29 ± 0.15
$[OII]\lambda 3727 [10^{-16} \text{ergs cm}^{-2} \text{s}^{-1}]$	35.25 ± 0.2	9.3 ± 0.8
$[OIII]\lambda 5008 [10^{-16} \text{ergs cm}^{-2} \text{s}^{-1}]$	9.33 ± 0.1	2.1 ± 0.2
$12 + \log(\text{O}/\text{H})[\text{O3N2}]^e$	$8.6 \pm 0.1 \pm 0.14$	$8.58 \pm 0.02 \pm 0.14$
$12 + \log(\text{O}/\text{H})[\text{N2}]^e$	$8.5 \pm 0.2 \pm 0.18$	$8.56 \pm 0.01 \pm 0.18$
$12 + \log(\text{O}/\text{H})[\text{R23}]^e$	$8.7 \pm 0.2 \pm 0.10$	$8.10 \pm 0.11 \pm 0.10$

^athis magnitude differs from the value (-21.0 ± 0.02) of König et al. (2006) in that we use Poggianti's kcorrection code and an internal extinction correction based on inclination and HI velocity width, while they use Blanton's kcorrection code (v3.2) Blanton & Roweis (2007) and correct for internal extinction using the Balmer-line ratio and the method of Cardelli et al. (1989)

^busing colors from Holmberg et al. (2006) and converting to AB zeropoint with Frei & Gunn (1994)

^cdereddened luminosity

^dnuclear HI column density derived from $SFR_{H\alpha}$

^ethe two errors listed are our measured error and the systematic error in the calibration for each of the three techniques used, respectively

Table 3: HI properties of Mrk 1456, SDSS 21-00, and Mrk 1457

Galaxy	Sdv [$K \cdot (km s^{-1})$]	W_{50} [$km s^{-1}$]	W_{20} [$km s^{-1}$]	v_{sys} [$km s^{-1}$]	M_{HI} [$10^9 M_{\odot}$]	M_{HI}^*	M_{dyn} [$10^{11} M_{\odot}$]	$\frac{M_{HI}}{L_B}$	$\frac{M_{dyn}}{L_B}$	$\frac{M_{HI}}{M_{dyn}}$
Mrk 1456	1.0808±0.0016	271.3	322.53	14262.1	5.64±0.002	0.89	0.9±0.4	0.30±0.02	4.8±0.6	0.062±0.006
SDSS 21-00	–	255.6	281.8	17357.7	13.6±0.3	2.03	0.69±0.15	1.2±0.1	6.1±0.9	0.20±0.03
Mrk 1457	1.0953±0.0012	294.1	344.94	14631.1	5.97±0.02	0.94	2.1±0.7	0.14±0.01	5.0±0.4	0.029±0.002

¹measurements made using Gmeasure mode 2, which takes 20% or 50% of the highest peak, and all properties calculated using the W_{50} velocity width

Table 4: Properties of the Mrk 1456 & 'SDSS 21-00' Galaxy Group

Group	COM [hh:mm:ss, dd:mm:ss]	COM v_{rad} [km s^{-1}]	W [km s^{-1}]	M_{vir} [$10^{13} M_{\odot}$]	No. of Members	R_{vir} [Mpc]
Mrk 1456	11:47:23.76, +52:27:32.40	14390.04	172.275	0.7352	4	0.3551
SDSS J211701.26-002633.7	21:17:18.96, -00:21:14.40	17339.520	70.697	0.3911	7	1.1219

¹table lists overall group properties from (Merchán & Zandivarez 2005):
columns are group coordinates, group systematic velocity, group velocity width, virial mass, # of members, and virial radius

Table 5: Properties of Groups Members

Mrk 1456 Galaxy Group								
Members	Ra [hh:mm:ss]	Dec [dd:mm:ss]	v_{sys} [km s^{-1}]	z	b	b_{COM}^a [']	Type	u-r
Mrk 1456	11:47:20.20	+52:29:18.60	14261±24	0.04757±0.00008	—	1.9	Sc	1.47
Mrk 1457	11:47:21.61	+52:26:58.31	14562±28	0.04857±0.00009	2.3	0.7	Sy2	1.94
Mrk 1458	11:47:41.67	+52:26:55.88	14431±27	0.04814±0.00009	4.0	2.8	Sa	2.29
SDSS J114711.09+522653.4	11:47:11.10	+52:26:53.40	14308±46	0.0477±0.0002	2.8	2.0	E/S0	2.57
SDSS J211701.26-002633.7 Galaxy Group								
Members	Ra [hh:mm:ss]	Dec [dd:mm:ss]	v_{sys} [km s^{-1}]	z	b	b_{COM}^a [']		
SDSS J211701.26-002633.7	21:17:01.27	-00:26:33.80	17363±27	0.05792±0.00009	—	6.9	Sbc	1.69
SDSS J211716.84-002715.6	21:17:16.85	-00:27:15.60	17423±28	0.05812±0.00009	4.0	6.0	Sbc	1.83
SDSS J211715.44-002435.5	21:17:15.44	-00:24:35.50	17310±40	0.0577±0.0001	4.1	3.5	E/S0	2.60
SDSS J211709.94-003028.3	21:17:09.94	-00:30:28.30	17365±17	0.05792±0.00006	4.5	9.5	Sc	1.41
SDSS J211723.72-001845.9	21:17:23.72	-00:18:45.90	17391±16	0.05801±0.00005	9.6	2.7	Sbc	1.97
SDSS J211731.47-001246.9	21:17:31.47	-00:12:46.90	17308±46	0.0577±0.0002	15.7	9.0	S0	2.70
SDSS J211733.50-000805.0	21:17:33.50	-00:08:05.00	17217±19	0.05743±0.00007	20.2	13.7	Sc	2.09

^adistance from Center of Mass of the group